Report on historical simulations (T1.3)

Deliverable 1.8

Authors: Nicolas Gruber, Stephen Sitch

This project received funding from the Horizon 2020 programme under the grant agreement No. 821003.

Document Information

GRANT AGREEMENT	821003
PROJECT TITLE	Climate Carbon Interactions in the Current Century
PROJECT ACRONYM	4C
PROJECT START DATE	1/6/2019
RELATED WORK PACKAGE	WP1
RELATED TASK(S)	T1.3
LEAD ORGANIZATION	ETHZ
AUTHORS	Nicolas Gruber, Stephen Sitch
SUBMISSION DATE	05.11.2022
DISSEMINATION LEVEL	CO

History

DATE	SUBMITTED BY	REVIEWED BY	VISION (NOTES)
05.11.2022	ETHZ (Gruber)		
08.11.2022		UNEXE (Friedlingstein)	

Please cite this report as: Gruber, NP, Sitch, S (2022), Report on historical simulations, D1.8 of the 4C project

Table of Contents

List of figures

No table of figures entries found.

About 4C

Climate-Carbon Interactions in the Coming Century (4C) is an EU-funded H2020 project that addresses the crucial knowledge gap in the climate sensitivity to carbon dioxide emissions, by reducing the uncertainty in our quantitative understanding of carbon-climate interactions and feedbacks. This will be achieved through innovative integration of models and observations, providing new constraints on modelled carbon-climate interactions and climate projections, and supporting Intergovernmental Panel on Climate Change (IPCC) assessments and policy objectives.

Executive Summary

The 4C team coordinated the Global Carbon Budget 2021 (GCB2021) and latest GCB2022 (published 11 Nov 2022, at COP27), including analysing and summarising data from each component of the budget, writing and submission of the manuscript to ESSD (Friedlingstein et al., 2021, 2022), and data dissemination. 4C partners were among the core leaders that generated the updated ocean and land model simulations used in the 2021 and 2022 annual update of the Global Carbon Budget as described in this deliverable.

Keywords

Ocean carbon-cycle, Global Ocean Biosphere models, Land carbon-cycle, Dynamic Global Vegetation Models, Earth System Models.

1 Introduction

This document provides the description of how task 1.3 of the EU H2020 project 4C was accomplished and represents the project deliverable D1.8.

The goals of task 1.3 as given in the grant agreement are “Simulating the global carbon cycle from 1900 to 2020. In T1.3, a series of model simulations will be performed using the latest CMIP6+ model improvements and forcing on an annual basis. This includes historical simulations with the land and ocean carbon models, forced by the observed atmospheric conditions of the 120 years. The uncertainty associated with the atmospheric forcing will be investigated by using different reconstructions of the atmospheric state. T1.3 includes also historical simulations with the 4C ESMs in emission-driven mode.”

Detailed protocols were generated for both land and ocean models simulations (see section 2). Extended model simulations with additional data requirements and forcing specifications were requested, which are used in the REgional Carbon Cycle Assessment and Processes 2 project (RECCAP-2) that is underway. Land simulations this year (for GCB2022) includes revised land-use and land cover change maps. The assessment of the ocean simulations now includes a much larger set of ocean data products.

Key Publication:

Friedlingstein et al., Global Carbon Budget 2022, ESSD, doi:

2 Historical simulations of carbon cycle models

2.1 Global Ocean Biosphere Models (GOBMs)

4C partners have produced new historical ocean model simulations, run up to 2021, and used in the annual update of the GCB (Friedlingstein et al., 2021). The mean and spread of the annual global carbon flux for these models is shown in Figure 1. Factorial simulations have been run for each model to isolate the forcing variables of anthropogenic atmospheric CO2 (Fig. 1 b) and climate (Fig. 1 c). The NEMO-PlankTOM12 (low-resolution) model, from the UEA group (shown in cyan in Figure 1), has also been used for a number of external-forcing experiments to test the sensitivity of the simulated carbon flux. The experiments changed the model forcing reanalysis product from NCEP to JRA55, ERA5 and METO, as well as isolating the wind speed and wind stress elements of NCEP. They show that forcing has an important effect for the specific variability of the CO2 sink, with the largest impact in the Southern Ocean. The NEMO-PlankTOM12 high-resolution model has progressed so that it can be run with the full physics setup, but not yet the biogeochemistry.

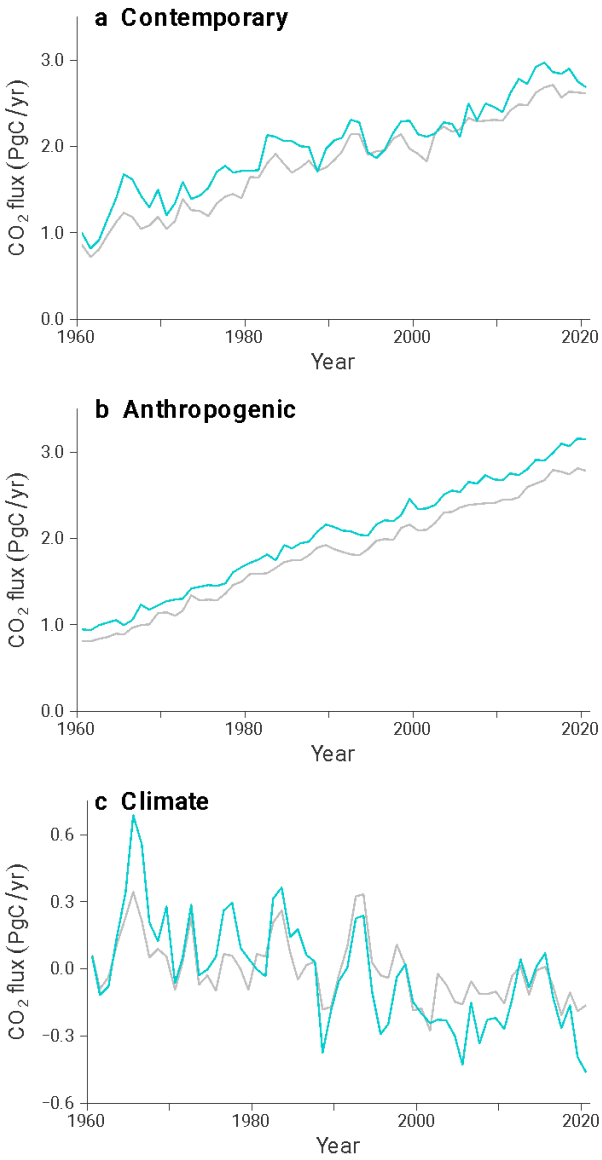

Figure 1: Annual global oceanic CO2 flux from global ocean biogeochemistry models used in the Global Carbon Budget 2022 (REF), for the multi-model mean and ±1 standard deviation (grey line and shading) and for the NEMO-PlankTOM12 model (cyan line). Carbon is partitioned into (a) contemporary (from increasing atmospheric CO2, climate change, and climate variability), (b) anthropogenic (from increasing atmospheric CO2 only), and (c) climate (from climate change and climate variability, calculated as the difference between contemporary and anthropogenic carbon).

Historical simulations GCB2022

The ocean CO2 sink for 1959-20121 is estimated using ten GOBMs. The GOBMs represent the physical, chemical, and biological processes that influence the surface ocean concentration of CO2 and thus the air-sea CO2 flux. The GOBMs are forced by meteorological reanalysis and atmospheric CO2 concentration data available for the entire time period.

Four sets of simulations were performed with each of the GOBMs. Simulation A applied historical changes in climate and atmospheric CO2 concentration. Simulation B is a control simulation with constant atmospheric forcing (normal year or repeated year forcing) and constant pre-industrial atmospheric CO2 concentration. Simulation C is forced with historical changes in atmospheric CO2 concentration, but repeated year or normal year atmospheric climate forcing. Simulation D is forced by historical changes in climate and constant pre-industrial atmospheric CO2 concentration. To derive SOCEAN from the model simulations, we subtracted the slope of a linear fit to the annual time series of the control simulation B from the annual time series of simulation A. Assuming that drift and bias are the same in simulations A and B, we thereby correct for any model drift.

Key Results from GCB 2022 GOBM historical simulations:

Cumulated since 1850, the ocean sink adds up to 175 ± 35 GtC, with more than two thirds of this amount (120 GtC) being taken up by the global ocean since 1960. Over the historical period, the ocean sink increased in pace with the anthropogenic emissions exponential increase. Since 1850, the ocean has removed 26% of total anthropogenic emissions.

The ocean CO2 sink increased from 1.1 ± 0.4 GtC yr-1 in the 1960s to 2.9 ± 0.4 GtC yr-1 during 2012-2021, with interannual variations of the order of a few tenths of GtC yr-1 (Figure 2). The ocean-borne fraction (SOCEAN/(EFOS+ELUC) has been remarkably constant around 25% on average.

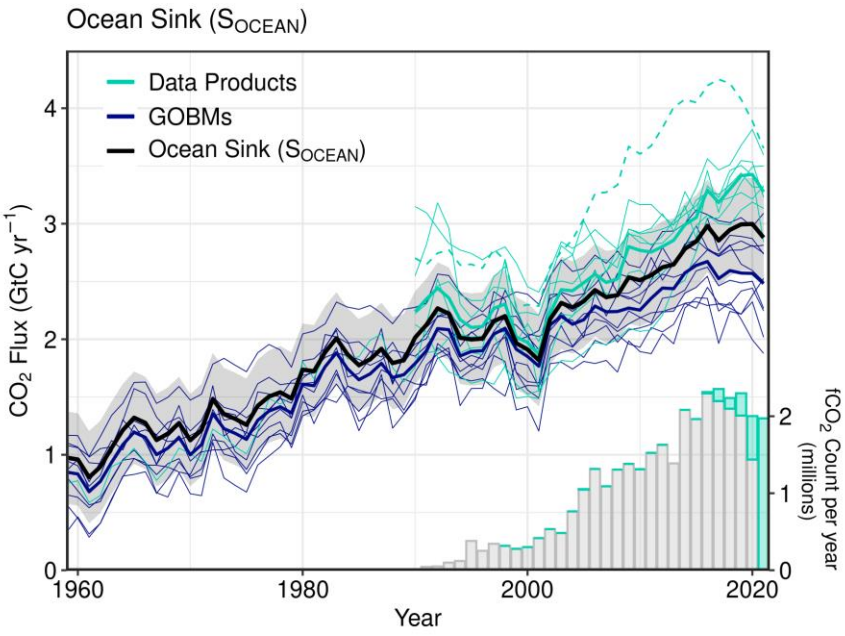

Figure 2. Comparison of the anthropogenic atmosphere-ocean CO2 flux showing the budget values of SOCEAN (black; with the uncertainty in grey shading), individual ocean models (royal blue), and the ocean fCO2-based data products (cyan; with Watson et al. (2020) in dashed line as not used for ensemble mean). Only one data product (Jena-MLS) extends back to 1959 (Rödenbeck et al., 2022). The fCO2-based data products were adjusted for the pre-industrial ocean source of CO2 from river

input to the ocean, by subtracting a source of 0.65 GtC yr-1 to make them comparable to SOCEAN . Bar-plot in the lower right illustrates the number of fCO2 observations in the SOCAT v2022 database (Bakker et al.,2022). Grey bars indicate the number of data points in SOCAT v2021, and coloured bars the newly added observations in v2022.

The increase of the ocean sink is primarily driven by the increased atmospheric CO2 concentration, with the strongest CO2 induced signal in the North Atlantic and the Southern Ocean (Figure 3a). The effect of climate change is much weaker, reducing the ocean sink globally by 0.11 ± 0.09 GtC yr-1 (-4.2%) during 2012-2021 (nine models simulate a weakening of the ocean sink by climate change, range -3.2 to -8.9%, and only one model simulates a strengthening by 4.8%), and does not show clear spatial patterns across the GOBMs ensemble (Figure 3b). This is the combined effect of change and variability in all atmospheric forcing fields, previously attributed to wind and temperature changes in one model (LeQuéré et al., 2010).

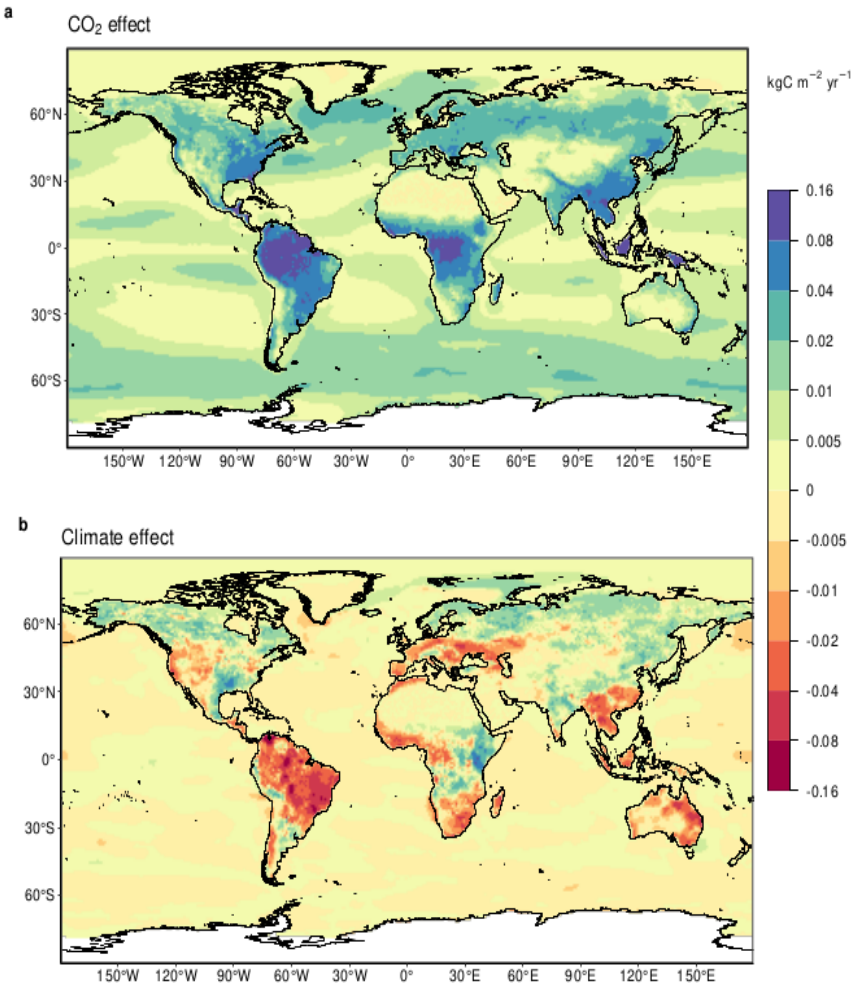

Figure 3. Attribution of the atmosphere-ocean (S_{OCEAN}) and atmosphere-land (S_{LAND}) CO_2 fluxes to (a) increasing atmospheric CO_2 concentrations and (b) changes in climate, averaged over the previous decade 2012-2021. All data shown is from the processed-based GOBMs and DGVMs. Units are in kgC m^{-2} yr^{-1} (note the non-linear colour scale).

2.2 Dynamic Global Vegetation Models (DGVMs)

We assembled the forcing datasets (incl. climate, CO2 and land-use) and developed the simulation protocol used for TRENDYv10 /GCB 2021 and 2022. This included updated forcing based on the analyses of Rosan et al., 2021 (land-use) and O'Sullivan et al., 2021 (improved radiation fields).

The land carbon models were be forced over the period 1700-2020 (GCB 2020), with historical observed atmospheric CO2 from a global network of monitoring stations, changing climatology (6-hourly JRA model reanalysis aligned with CRU observation-based monthly climatology from 1900), land-use and land cover changes (LUH2), and derived nitrogen deposition, fertiliser and manure application, following the TRENDY protocol. The following 4C land carbon models (with host ESM in parenthesis) participated in GCB2021 and GCB2022 using their CMIP6+ configuration: JULES, ORCHIDEE (IPSL-ESM), LPX (BERN3D-LPX), LPJ-GUESS (EC-Earth ESM), JSBACH (MPI-ESM).

Following GCB2021 and in preparation for GCB2022 we critically assessed our land-use datasets leading to modified methodologies and data for several countries, including Brazil and the Democratic Republic of Congo (DRC). In Brazil deforestation was in decline from its historical peak in 2004, but had begun to pick-up in the last years. This increase in deforestation was not being picked up in our methodology where we rely on the FAO agriculture reporting to 2017, and then extrapolate in time using a simple trend. Furthermore, Rosan et al., 2021 showed how the FAO agriculture area change may be systematically lower than area deforested (FAO has a further "other land" category not used in the HYDE land-use model), leading us to believe that we may be underestimating land-use change emissions for Brazil. To resolve these two issues we incorporated the agricultural area data from an alternative in-country land-use dataset, mapbiomas, within HYDE land-use model (Figure 4). For DRC there appears an explained change in land-use in 2010. The DRC data has recently been retrospectively updated by FAO, and the new data incorporated into the HYDE land-use model (Figure 4). HYDE uses state or country-level agricultural total area data to generate a spatially gridded product which is then used by LUH2 to generate land-use transitions. These new LULCC forcing datasets were used as input to global bookkeeping models and DGVMs to estimate the carbon emissions due to land-use change in GCB2022.

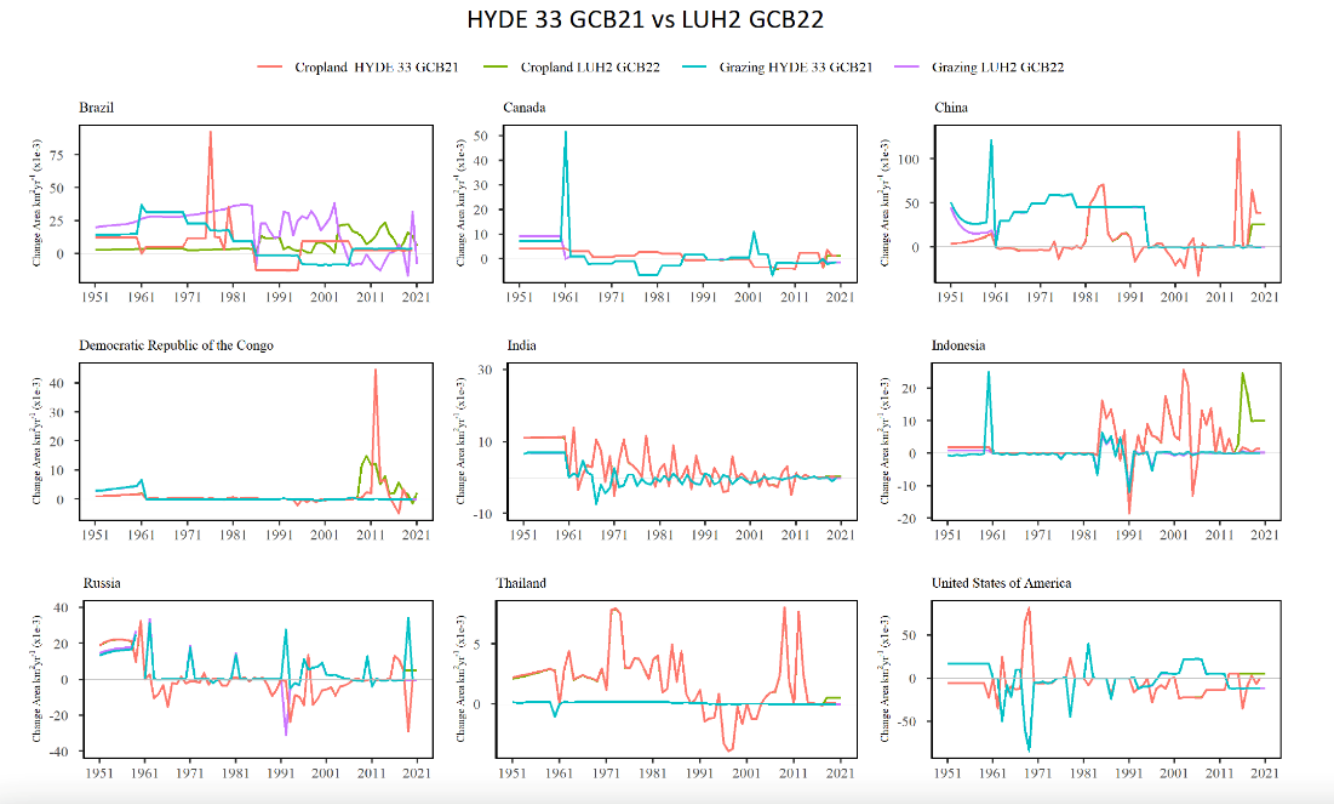

Figure 4. Country-level agricultural area changes used in GCB 2021 (red =cropland; light blue grazing land), and GCB 2022 (green = cropland; purple grazing land). Note the large changes in Brazil and in 2010 in the DRC.

Historical simulations GCB2022

DGVMs were forcing data include time dependent gridded climate forcing, global atmospheric CO2, gridded land cover changes (see above), and gridded nitrogen deposition and fertilisers. Four simulations were performed with each of the 16 DGVMs. Simulation 0 (S0) is a control simulation which uses fixed pre-industrial (year 1700) atmospheric CO2 concentrations, cycles early 20th century (1901-1920) climate and applies a time-invariant pre-industrial land cover distribution and pre-industrial wood harvest rates. Simulation 1 (S1) differs from S0 by applying historical changes in atmospheric CO2 concentration and N inputs. Simulation 2 (S2) applies historical changes in atmospheric CO2 concentration, N inputs, and climate, while applying time-invariant pre-industrial land cover distribution and pre-industrial wood harvest rates. Simulation 3 (S3) applies historical changes in atmospheric CO2 concentration, N inputs, climate, and land cover distribution and wood harvest rates.

S2 is used to estimate the land sink component of the global carbon budget (SLAND). S3 is used to estimate the total land flux but is not used in the global carbon budget. We further separate SLAND into contributions from CO2 (=S1-S0) and climate (=S2-S1+S0).

Key Results from GCB 2022 DGVM historical simulations:

Cumulated since 1850, the terrestrial CO2 sink amounts to 210 ± 45 GtC, 31% of total anthropogenic emissions. Over the historical period, the sink increased in pace with the anthropogenic emissions exponential increase. The terrestrial CO2 sink increased from 1.2 ± 0.4 GtC yr-1 in the 1960s to 3.1 ± 0.6 GtC yr-1 during 2012-2021, with important interannual variations of up to 2 GtC yr-1 generally showing a decreased land sink during El Niño events (Figure 5), responsible for the corresponding enhanced growth rate in atmospheric CO2 concentration. The larger land CO2 sink during 2012-2021 compared to the 1960s is reproduced by all the DGVMs in response to the increase in both atmospheric CO2 and nitrogen deposition, and the changes in climate, and is consistent with constraints from the other budget terms.

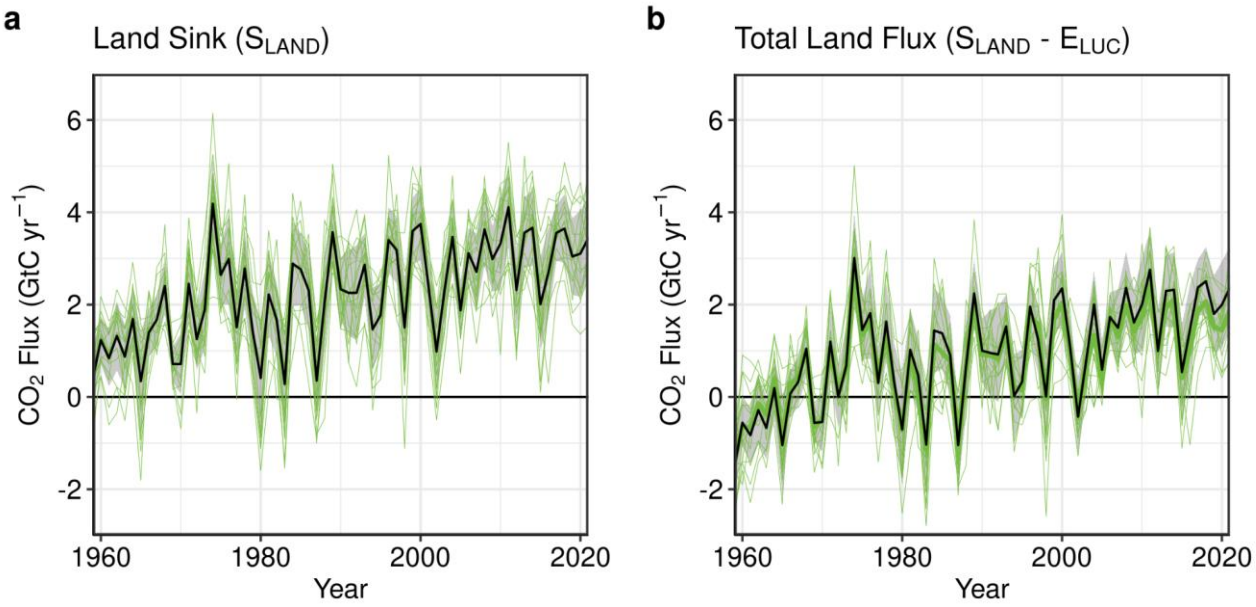

Figure 5: (a) The land CO2 sink (SLAND) estimated by individual DGVMs estimates (green), as well as the budget estimate (black with ±1σ uncertainty), which is the average of all DGVMs. (b) Total atmosphere-land CO2 fluxes (SLAND – ELUC). The budget estimate of the total land flux (black with ±1σ uncertainty) combines the DGVM estimate of SLAND from panel (a) with the bookkeeping estimate of ELUC from Figure 7(a). Uncertainties are similarly propagated in quadrature from the budget estimates of SLAND from panel (a) and ELUC from Figure 7(a). DGVMs also provide estimates of ELUC which can be combined with their own estimates of the land sink. Hence panel (b) also includes an estimate for the total land flux for individual DGVMs (thin green lines) and their multi-model mean (thick green line).

Over the period 1960 to present the increase in the global terrestrial CO2 sink is largely attributed to the CO2 fertilisation effect (Prentice et al., 2001), directly stimulating plant photosynthesis and increased plant water use in water limited systems, with a small negative contribution of climate change (Figure 3). There is a range of evidence to support a positive terrestrial carbon sink in response to increasing atmospheric CO2, albeit with uncertain magnitude (Walker et al., 2021). As expected from theory, the greatest CO2 effect is simulated in the tropical forest regions, associated with warm temperatures and long growing seasons (Hickler et al., 2008) (Figure 3a). During 2012-2021 the land sink is positive in all regions with the exception of eastern Brazil, Southwest USA, Southeast Europe and Central Asia, North and South Africa, and eastern Australia, where the

negative effects of climate variability and change (i.e. reduced rainfall) counterbalance CO2 effects. This is clearly visible on Figure 3 where the effects of CO2 (Figure 3a) and climate (Figure 3b) as simulated by the DGVMs are isolated. The negative effect of climate is the strongest in most of South America, Central America, Southwest US, Central Europe, western Sahel, southern Africa, Southeast Asia and southern China, and eastern Australia (Figure 3b). Globally, climate change reduces the land sink by 0.63 ± 0.52 GtC yr-1 or 17% (2012-2021).

2.3 4C ESMs in emission-driven mode

We performed historical simulations of the global carbon cycle using ESMs. Description of work achieved is given here for the EC-Earth3 ESM, and present results from the esm-hist (CO2 emission-driven) and historical (CO2 concentration-driven) simulations of the EC-Earth3-CC model, the carbon-cycle version. BSC has produced during this reporting period 9 additional historical and esm-hist simulations, starting from different periods of the piControl and esm-piControl simulations, respectively. The esm-hist simulations were done with an improved treatment of the surface-atmosphere flux which did not significantly change global average surface atmospheric CO2. In Figure 6 we show the globally-averaged CO2 concentrations of the EC-Earth-CC esm-hist simulation, compared to CO2 concentrations from the NOAA/input4MIPs dataset. EC-Earth-CC shows a positive bias developing after 1920, which reaches a value of about +30 ppm at the end of the historical period (2014). This bias is slightly higher in the member which started from 1850 of the esm-piControl, compared to the other members which started from lower initial CO2 values. This bias puts EC-Earth-CC at the upper-end of the CMIP5 models, none of which exhibits the flat growth in CO2 from 1940 to 1960 seen in observations.

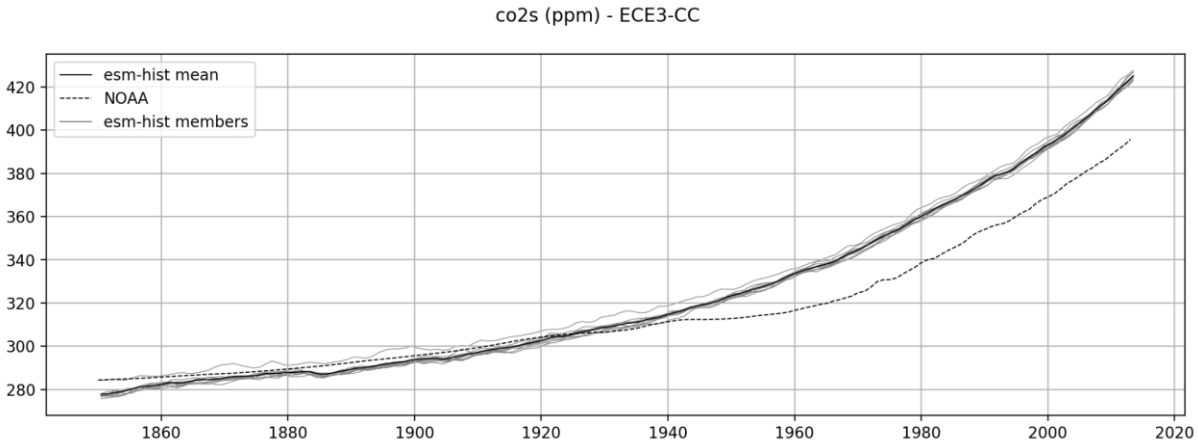

Figure 6. Globally-averaged surface CO2 concentration (in ppm) of the EC-Earth-CC esm-hist simulation (10-member ensemble mean in black, individual members in gray), compared to globally-averaged observed CO2 concentration from NOAA/input4MIPS (dashed black).

In Figure 7 we show the 10-member ensemble means of accumulated global sum of atmosphere-land and atmosphere-ocean carbon fluxes. Accumulated land carbon loss is about 90 Pg in the historical and 105 Pg in

the esm-hist simulations, both of which are quite large when compared to observational estimates and other carbon-cycle models, but still within the large range of CMIP5 model simulations (107 to -170 PgC). These values are slightly improved over those presented in the single-model simulation presented in the first periodic report of the 4C project. The lower carbon loss in the esm-hist simulation is due to CO2 fertilization, given that the atmospheric CO2 is higher than in the historical simulations.

In contrast, ocean uptake during the historical period is approximately 150 PgC in the historical simulation and 190 PgC in the esm-hist simulation. In the historical simulation, driven by observed CO2, carbon uptake by the ocean is accurately simulated compared to observations and CMIP5 models. The positive bias in carbon uptake in the esm-hist is attributed to the positive bias in CO2 (from land processes) which increases atmospheric-ocean carbon fluxes. In this case the values are nearly identical to the single-member results presented in the previous report.

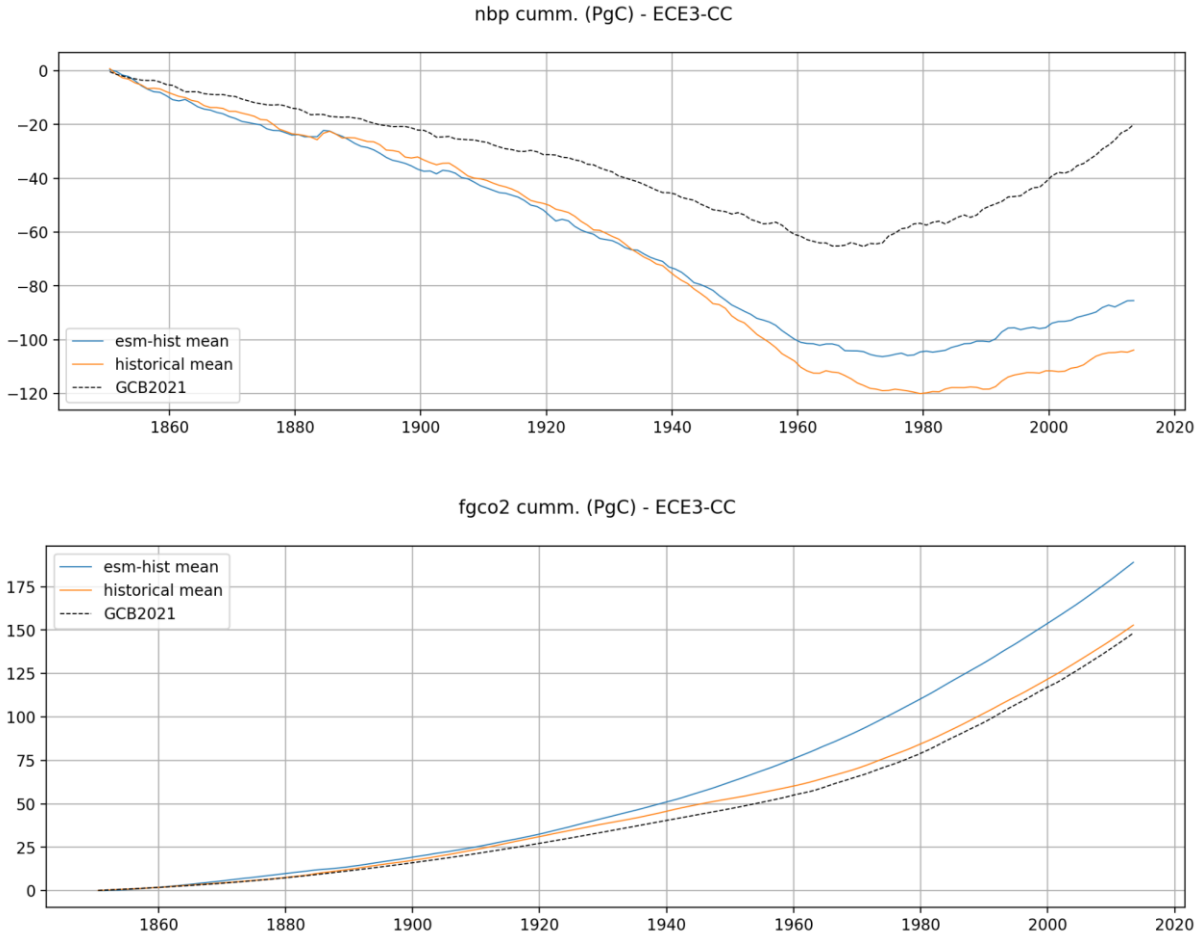

Figure 7. Accumulated global sum of CO2 fluxes (in PgC) from atmosphere-land (top, nbp) and atmosphere-ocean (bottom, fgco2) in the ensemble mean of the 10 EC-Earth-CC esm-hist (blue) and historical (orange) simulations, compared to estimates from GCB2021. Positive values indicate carbon uptake by the land/ocean.

3 Summary

GOBMs and DGVMs were applied over the historical period with results analysed and published in GCB. Key findings relating to the contemporary ocean and land carbon budgets are summarised as follows:

The ocean CO2 sink resumed a more rapid growth in the past two decades after low or no growth during the 1991-2002 period. However, the growth of the ocean CO2 sink in the past decade has an uncertainty of a factor of three, with estimates based on data products and estimates based on models showing an ocean sink trend of +0.7 GtC yr-1 decade-1 and +0.2 GtC yr-1 decade-1 since 2010, respectively. The discrepancy in the trend originates from all latitudes but is largest in the Southern Ocean. The ocean CO2 sink was 2.9 ± 0.4 GtC yr-1 during the decade 2012-2021 (26% of total CO2 emissions), with a similar preliminary estimate of 2.9 GtC yr-1 for 2022.

The land CO2 sink continued to increase during the 2012-2021 period primarily in response to increased atmospheric CO2, albeit with large interannual variability. The land CO2 sink was 3.1 ± 0.6 GtC yr-1 during the 2012-2021 decade (29% of total CO2 emissions), 0.4 GtC yr-1 larger than during the previous decade (2000-2009), with a preliminary 2022 estimate of around 3.4 GtC yr-1. Year to year variability in the land sink is about 1 GtC yr-1 and dominates the year-to-year changes in the global atmospheric CO2 concentration, implying that small annual changes in anthropogenic emissions (such as the fossil fuel emission decrease in 2020) are hard to detect in the atmospheric CO2 observations.

4 References

Bakker et al., Surface Ocean CO2 Atlas Database Version 2022 (SOCATv2022) (NCEI Accession 0253659). NOAA National Centers for Environmental Information. https://doi.org/10.25921/1h9f-nb73.

Friedlingstein et al., Global Carbon Budget 2022, ESSD, doi:

Friedlingstein et al., Global Carbon Budget 2020, Earth Syst. Sci. Data, 12, 3269–3340, https://doi.org/10.5194/essd-12-3269-2020, 2020.

Hickler et al., CO2 fertilization in temperate FACE experiments not representative of boreal and tropical forests, 14, 1531–1542, https://doi.org/10.1111/j.1365-2486.2008.01598.x, 2008.

LeQuéré et al., Impact of climate change and variability on the global oceanic sink of CO2, Global Biogeochem. Cy., 24,GB4007, https://doi.org/10.1029/2009GB003599, 2010.

O'Sullivan et al., Aerosol–light interactions reduce the carbon budget imbalance, Environ. Res. Lett., 16, 124072, https://doi.org/10.1088/1748-9326/ac3b77, 2021.

Prentice et al., The Carbon Cycle and Atmospheric Carbon Dioxide, in Climate Change 2001: The Scientific Basis. Contribution of Working Group I to the Third Assessment Report of the Intergovernmental Panel on Climate Change, edited by: Houghton, J. T., Ding, Y., Griggs, D. J., Noguer, M., van der Linden, P. J., Dai, X., Maskell, K., and Johnson, C. A., Cambridge University Press, Cambridge, United Kingdom and New York, NY, USA, 183–237, 2001.

Rödenbeck et al., Data-based estimates of interannual sea–air CO2 flux variations 1957–2020 and their relation to environmental drivers, Biogeosciences, 19, 2627–2652, https://doi.org/10.5194/bg-19-2627-2022, 2022.

Rosan et al., A multi-data assessment of land use and land cover emissions from Brazil during 2000–2019, Environ. Res. Lett., 16, 074004, https://doi.org/10.1088/1748-9326/ac08c3, 2021.

Walker et al., Integrating the evidence for a terrestrial carbon sink caused by increasing atmospheric CO2, 229, 2413–2445, https://doi.org/10.1111/nph.16866, 2021.

Watson et al. Revised estimates of ocean-atmosphere CO2 flux are consistent with ocean carbon inventory, Nat Commun, 11, 4422, https://doi.org/10.1038/s41467-020-18203-3, 2020.